

Visualization of Weak Interaction Effects on N₂O Schiff Base Ligands in Iron(II) Spin Crossover Complexes

Kunihisa Sugimoto^{†, ‡}, Takashi Okubo[§], Masahiko Maekawa[§], Takayoshi Kuroda-Sowa[§]*

[†]Diffraction & Scattering Division, Japan Synchrotron Radiation Research Institute (JASRI), 1-1-1 Kouto, Sayo-cho, Sayo-gun, Hyogo 679-5198 Japan; [‡]Institute for Integrated Cell-Material Sciences (iCeMS), Institute for Advance Study, Kyoto University, Yoshida-Honmachi, Sakyo-ku, Kyoto 606-8501 Japan; [§]Department of Chemistry, Faculty of Science and Engineering, Kindai University, Higashi-Osaka, Osaka 577-8502 Japan.

*ksugimoto@spring8.or.jp, sugimoto.kunihisa.4s@kyoyo-u.ac.jp

KEYWORDS. Iron(II) Schiff base complexes; Spin crossover; Single crystal; Hydrogen Bonding; Synchrotron Radiation.

ABSTRACT

Single crystals of an iron(II) spin crossover (SCO) complex containing an N₂O Schiff base ligand, [Fe^{II}(qsal-COOH)₂], were successfully prepared. The crystal structures from a single-crystal X-ray diffraction study were obtained at 100 and 170 K, and yielded information

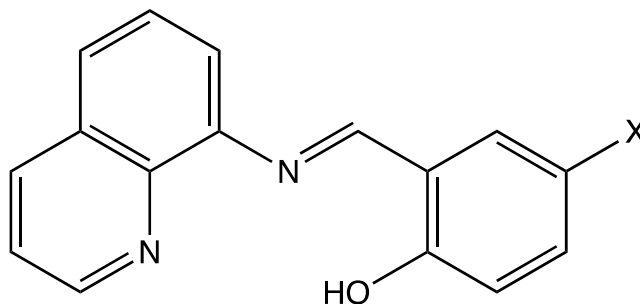
regarding both the low-spin and high-spin phases, without any crystal breakage being observed after the phase transition. Structural analysis was performed to visualize the origin of the SCO phenomenon in the $[\text{Fe}^{\text{II}}(\text{qsal-COOH})_2]$ complex. We report that the fundamental requirements for an abrupt SCO, particularly in Fe-qsal complexes, are not only a combination of weak interaction effects such, as π - π , P4AE (parallel fourfold aryl embrace), and hydrogen bonding, but also the presence of solvents in the crystalline structure, since the solvent molecules can influence the interactions between the $[\text{Fe}^{\text{II}}(\text{qsal-X})_2]$ molecules.

INTRODUCTION

Transition metal compounds containing Schiff base ligands are of particular importance in the domain of coordination chemistry, such as in the context of catalysts for the epoxidation of olefins, and for use in Michael addition reactions, among others.¹ An attractive function of transition metal compounds containing Schiff base ligands is the spin crossover (SCO) phenomenon. As a result, considerable efforts have been devoted to finding a new SCO system to understand the mechanisms of spin transitions, which could lead to their application in areas such as optoelectronics and memory devices.²⁻⁴ The SCO phenomenon can be applied to molecule-based materials because it is relatively easy to switch using external fields, and as a result, it has been actively studied. For example, molecules exhibiting abrupt spin transitions have attracted significant attention owing to not only the obvious abruptness of the transition, but also the wide hysteresis, both of which are important factors in realizing novel devices. These features are strongly correlated to the intermolecular interactions present in the system, such as coordination bonds,^{5,6} hydrogen bonds,⁷ and π - π interactions.^{8,9} The stimuli caused by structural changes in one SCO center can then propagate to neighboring centers through such interactions, and this is known as the cooperative effect or the domino effect.

One Schiff base ligand, qsal (*N*-(8'-quinoly)l)-2-hydroxy-1-salicylalimine), shown in Scheme 1, has been extensively studied in the context of Fe^{II} SCO complexes. The preparation and structural and magnetic properties of four Fe(II) Schiff base complexes, i.e., [Fe(qsal-X)₂] (X = F, Cl, Br, and I), have been previously reported.¹⁰⁻¹⁴ In addition, our group previously synthesized [Fe^{II}(qsal-COOH)₂] (**1**), an Fe(II) complex, which exhibits the SCO phenomenon with a hysteresis of 21 K, in which the ascending $\chi_{\text{M}}T$ value rapidly increases at 150 K, and the descending $\chi_{\text{M}}T$ value decreases sharply at 129 K, as determined by magnetic susceptibility measurements.¹³ Although we attempted to understand this magnetic phenomenon based on structural science, unfortunately, we were unable to prepare samples for single-crystal structure analysis.

Scheme 1. Structure of the qsal-X Schiff base ligand (X = F, Cl, Br, I, or COOH)



Thus, we herein report the preparation of single crystals of [Fe^{II}(qsal-COOH)₂] using methanol/water as the solvent, followed by subsequent X-ray structural analysis. In addition, the magnetic properties of the samples crystallized at different temperatures are compared in terms of their SCO behavior. To understand the mechanism of the SCO phenomenon of complex **1**, we perform single-crystal analysis for both the high-spin (HS) and low-spin (LS) phases, and the effects of the intermolecular interactions on the SCO properties are examined.

EXPERIMENTAL SECTION

General Procedures. All reagents and solvents of special grade chemicals were commercially available and were used as received unless otherwise stated. All preparations and manipulations were performed under an argon atmosphere using Schlenk techniques. Single crystals of **1** were obtained by crystallization at room temperature (**1-RT**) and at 323 K (**1-HT**).

Magnetic Studies. Magnetic susceptibility measurements in the temperature range of 2–400 K were carried out on fresh microcrystalline samples with applying magnetic field of 1 T, using a MPMSXL7 SQUID (Quantum Design) magnetometer. A diamagnetic correction to the observed susceptibilities was applied using Pascal's constants.

Single-crystal X-ray structure analysis. Measurements of complexes **1-RT** and **1-HT** were performed using a PILATUS3 X CdTe 1M detector (DECTRIS) at the SPring-8/BL02B1 beamline in Japan. The wavelengths ($\lambda = 0.4176 \text{ \AA}$ for **1-RT** and $\lambda = 0.4149 \text{ \AA}$ for **1-HT**) were selected using Si(311) monochromator crystals. Diffraction data were collected at 170 and 100 K for complexes **1-RT** and **1-HT**, respectively, using the ω scan mode. Data were collected and processed using the RAPID-AUTO program (Rigaku), and were corrected for Lorentz and polarization effects. Fortunately, even after the structural phase transition based on the SCO behavior, the single crystal of **1-HT** survived measurement at 100 K.

All structures were solved by direct methods (SHELXTL–2014)¹⁵ and were expanded using Fourier techniques. The non-hydrogen atoms were refined anisotropically (SHELXL–2017).¹⁶ The hydrogen atoms were refined using the AFIX command. To stabilize the refinement, the disordered methanol molecules were restrained to the same thermal displacement parameter and bond distances using the EADP and SADI commands for **1-HT** at 100 K. The total number of

occupancies for the disordered methanol molecules for **1-HT** at 100 K and the methanol and water molecules for **1-RT** at 170 and 100 K were restrained to 1.0 using the SUMP command. All calculations were performed using Olex2¹⁷ and ShelXle.¹⁸ The crystallographic data for complexes **1-RT** and **1-HT** are summarized in Tables S1 and S2, respectively. The atomic coordinates, bond lengths, and bond angles are listed in the CIF files, under CCDC 2024556, 2073267, 2073268, and 2073269.

RESULTS AND DISCUSSION

Magnetic properties and single-crystal X-ray structure analyses. The magnetic susceptibilities of the samples crystallized at room temperature (**1-RT**) and at 323 K (**1-HT**) showed different magnetic properties. The thermal variations of χ_{MT} for **1-RT** and **1-HT** are shown in Figures S1 and S2, respectively. As indicated, the magnetic susceptibility curve of **1-HT** was similar to that of **1**, with both exhibiting SCO properties. However, the magnetic properties of **1-RT** were able to maintain the high-spin (HS) state over all temperature ranges examined. We then analyzed single crystals of **1-RT** and **1-HT**, independent of the temperature, with the hypothesis that their different magnetic properties would be key to elucidating the origin of the SCO behavior. Thus, single-crystal X-ray structural analyses were performed at 100 and 170 K for **1-RT** and **1-HT**.

Complex **1-RT** was found to crystallize in the monoclinic C2/c space group, wherein the unit cell of **1-RT** contains crystallographically independent two molecules of $[\text{Fe}^{\text{II}}(\text{qsal-COOH})_2]$ and a solvent molecule of the disordered methanol and water, i.e., $[\text{Fe}^{\text{II}}(\text{qsal-COOH})_2] \cdot (\text{CH}_3\text{OH})_{0.5}(\text{H}_2\text{O})_{0.5}$. The Fe centers coordinate to the N_4O_2 donors of two tridentate qsal-COOH^- ligands chelating in a meridional fashion, as shown in Figure S3. The distances of

Fe–O and Fe–N in complex **1-RT** are between 2.073–2.076 and 2.178–2.237 Å at 170 K, respectively, and between 2.068–2.069 and 2.170–2.229 Å at 100 K, respectively. The structure of **1-RT** with Fe–L bond lengths of Fe–O_{ave.} = 2.075 and Fe–N_{ave.} = 2.206 Å at 170 K, and Fe–O_{ave.} = 2.068 and Fe–N_{ave.} = 2.197 Å at 100 K, is typical for Fe^{II} in the HS state. These measured bond lengths are therefore consistent with the magnetic susceptibility results for **1-RT**. In contrast, the crystal structures of **1-HT** obtained at 100 and 170 K yielded information regarding both the LS and HS phases. More specifically, complex [Fe^{II}(qsal-COOH)₂](CH₃OH) (**1-HT**) crystallizes in the monoclinic *P2₁/n* space group at both temperatures, thereby differing from **1-RT**. In addition, no symmetry breaking was observed during this phase transition. At both temperatures, the asymmetric units of **1-HT** contain a neutral molecule of [Fe^{II}(qsal-COOH)₂], which possesses a crystallographically independent Fe atom and two qsal-COOH molecules. In addition, the asymmetric unit of **1-HT** contains a neutral molecule of [Fe^{II}(qsal-COOH)₂], which possesses a crystallographically independent Fe atom, two qsal-COOH molecules, and one methanol solvent molecule. The Fe centers also coordinate to N₄O₂ donors from two tridentate qsal-COOH[−] ligands chelating in a meridional fashion, as shown in Figure 1. In the crystal structures of both **1-RT** and **1-HT**, the Fe centers coordinate to N₄O₂ donors from two tridentate qsal-COOH ligands chelating in a meridional fashion. The distances of Fe–O and Fe–N in complex **1-HT** at 170 K fall between 2.055–2.056 and 2.148–2.210 Å, respectively. The structure of **1-HT** at 170 K with Fe–L bond lengths of Fe–O_{ave.} = 2.0553 Å and Fe–N_{ave.} = 2.174 Å is typical of Fe^{II} in the HS state. The distances of Fe–O and Fe–N in complex **1-HT** at 100 K fall between 1.979–1.980 and 1.949–1.969 Å, respectively. The structure of **1-HT** at 100 K with Fe–L bond lengths of Fe–O_{ave.} = 1.9795 Å and Fe–N_{ave.} = 1.953 Å is typical of Fe^{II} in the LS state. The bond lengths of **1-HT** indicate that the Fe^{II} centers at 100 and 170 K are in the LS and

HS states, respectively. The results of these bond lengths are consistent with the magnetic properties of **1-HT**.

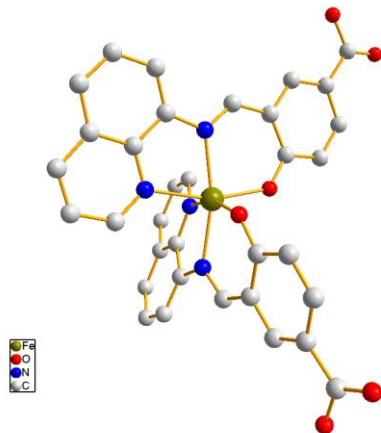


Figure 1. Molecular structure of **1-HT** at 170 K. Hydrogen atoms and methanol solvent molecules are omitted for clarity.

Crystal packing and intermolecular interactions. As mentioned above, the crystal structures of **1-HT** and **1-RT** belong to the monoclinic space group $P2_1/n$ and the $C2/c$ space group, respectively, wherein both crystallographic unit cells contain a $[\text{Fe}^{\text{II}}(\text{qsal-COOH})_2]$ molecule. As the overall packings in **1-HT** and **1-RT** were different, it was clear that the complex packings differed from those of typical $\text{Fe}^{\text{II}}\text{-qsal-X}$ complexes. According to reports by Murray et al.,¹⁰⁻¹⁴ a chain of Fe^{II} moieties interacts through $\pi\text{-}\pi$ and $\text{C-H}\cdots\pi$ interactions between the salicylidimine and quinoline rings of the qsal-X ligands. Moreover, $\text{C-X}\cdots\text{O}$ interactions and P4AE (parallel fourfold aryl embrace) interactions were found to link the Fe moieties into higher dimensions. However, the $[\text{Fe}^{\text{II}}(\text{qsal-COOH})_2]$ molecules in **1-HT** formed different pseudo-3D packing arrangements involving $\text{C-H}\cdots\text{O}$ interactions. More specifically, the pseudo-3D packing structure was formed by hydrogen bonding of the oxygen atoms originating from the hydroxyl

and carboxyl groups of salicylaldehyde, as shown in Figure 2. This results in intermolecular π — π interactions between the quinoline rings of the qsal-COOH ligands, which are similar to those observed in the molecular packing of $[\text{Fe}^{\text{II}}(\text{qsal-X})_2]$. However, no intermolecular C—H \cdots π interactions were found to be present in the quinoline rings of the qsal-COOH ligands, which is contrasting to the packing of Fe^{II} complexes consisting of qsal-X ligands bearing halogenated substituents.

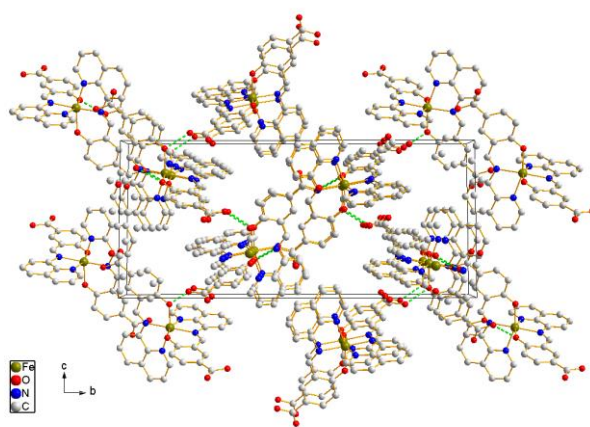


Figure 2. Perspective of the pseudo 3D packing structure of **1-HT** at 170 K formed by hydrogen bonding of the oxygen atoms originating from the hydroxyl and carboxyl groups of salicylaldehyde. Hydrogen bonds are represented by green dashed lines. Hydrogen atoms and methanol solvent molecules are omitted for clarity.

In contrast, the $[\text{Fe}^{\text{II}}(\text{qsal-COOH})_2]$ molecules in **1-RT** form double-chain structural arrangements involving C—H \cdots O interactions. One chain structure is formed by hydrogen bonding of the oxygen atoms originating from the hydroxyl and carboxyl groups of salicylaldehyde, similar to the case of **1-HT**. However, the other chain structure is formed by hydrogen bonding through the hydrogen atoms of the hydroxyl group of the methanol solvent molecules and the oxygen atoms of the hydroxyl and carboxyl groups of salicylaldehyde, as

shown in Figure 3. Thus, no intermolecular π — π or C—H \cdots π interactions were present. According to reports by W. Phonsri, in the $[\text{Fe}^{\text{III}}(\text{qsal-X})_2]$ complexes, hydrogen bonding through solvent molecules shows that intermolecular interactions have a dramatic effect on the properties of the SCO phenomenon.¹⁹

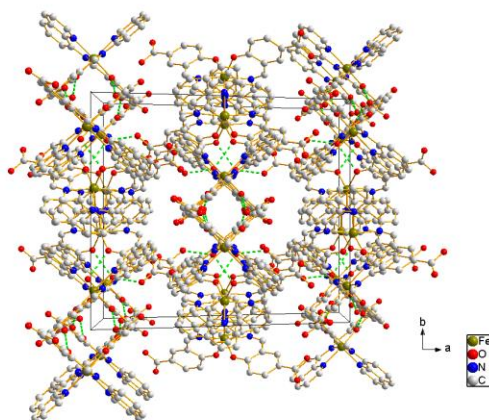


Figure 3. Perspective of the pseudo 3D packing structure of **1-RT** at 170 K formed by hydrogen bonding of the oxygen atoms originating from the hydroxyl and carboxyl groups of salicylaldimine. Hydrogen bonds are represented by green dashed lines. Hydrogen atoms and methanol solvent molecules are omitted for clarity.

At both temperatures, one of the qsal-COOH ligands in both complexes **1-RT** and **1-HT** was significantly distorted from the flat plane. More specifically, the dihedral angles between the salicylaldimine and quinoline rings in complex **1-HT** at 100 and 170 K were 28.19° for the LS phase and 28.85° for the HS phase, while the other dihedral angles were 6.80 and 9.74°, respectively, as shown in Figure 4. In contrast, in the crystal packing of **1-RT**, two crystallographically distinct $[\text{Fe}^{\text{II}}(\text{qsal-COOH})_2]$ molecules exist; the dihedral angles between the salicylaldimine and quinoline rings in complex **1-RT** for the HS phase at 100 and 170 K were

33.8 and 33.45°, respectively, while the other dihedral angles were 10.73 and 10.97°, respectively, as shown in Figure 5.

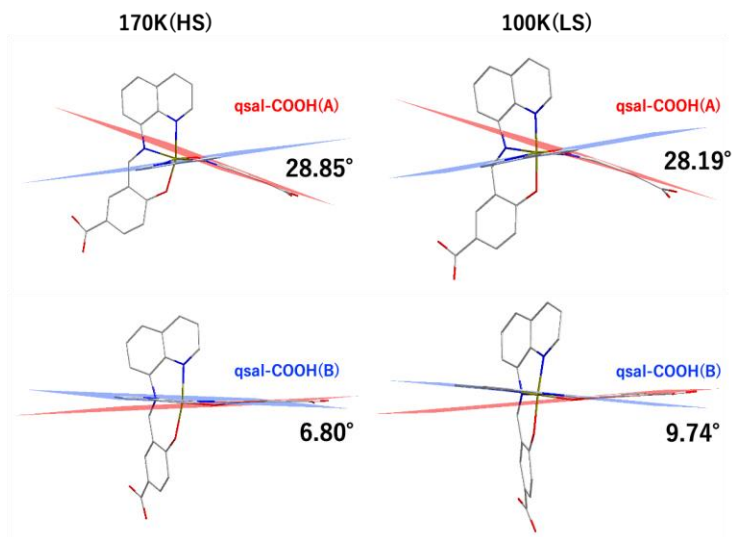


Figure 4. Dihedral angles between the salicylaldimine and quinoline rings in **1-HT** at 100 and 170 K.

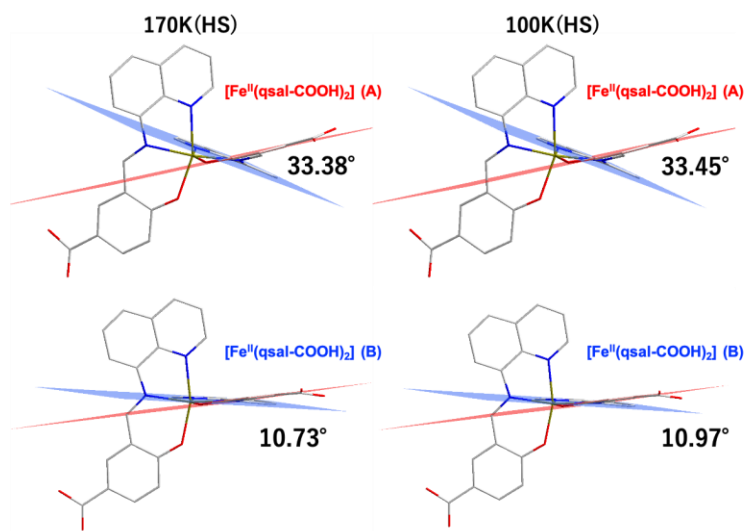


Figure 5. Dihedral angles between the salicylaldimine and quinoline rings in **1-RT** at 100 and 170 K. The labels of (A) and (B) show crystallographically independent molecules, respectively.

The large distortion angles can be accounted for by considering that a portion of the molecular packing of **1-HT** and **1-RT** forms a dimeric structure through C—H···O interactions, as shown in Figures 6 and 7, respectively. The magnetic property of **1-HT** corresponds to SCO behavior with a wide hysteresis >20 K, which is likely due to the hydrogen-bonding network originating from the carboxyl groups. However, **1-RT** maintains its HS state at low temperatures without SCO behavior, even in the presence of a hydrogen-bonding network between the [Fe^{II}(qsal-COOH)₂] molecules. This can be accounted for by considering that the main difference between **1-HT**, and **1-RT** is the crystallographic molecular symmetry of the [Fe^{II}(qsal-COOH)₂] molecule. More specifically, in the crystal packing of **1-RT**, the Fe^{II} atom is the inversion center of the [Fe^{II}(qsal-COOH)₂] molecule, and so it is possible that **1-RT** does not exhibit SCO behavior due to the fact that the distorted coordination environments around the Fe^{II} atoms are not anisotropic.

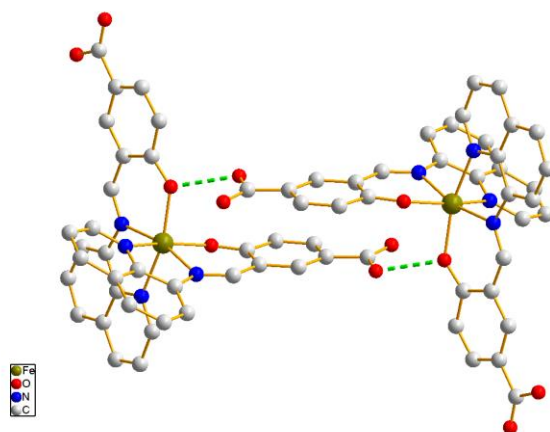


Figure 6. Part of the molecular packing of **1-HT** forms a dimeric structure through C—H···O interactions. Hydrogen bonds are represented by green dashed lines. Hydrogen atoms are omitted for clarity.

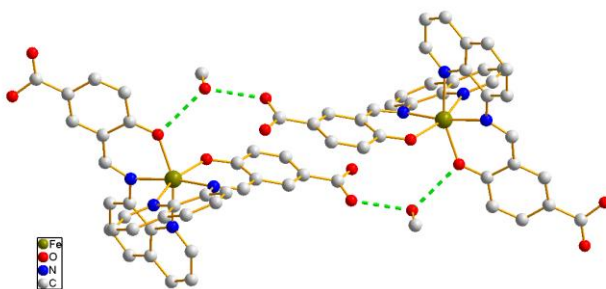


Figure 7. Part of the molecular packing of **1-RT** forms a dimeric structure through C—H···O interactions between the methanol solvent molecules. Hydrogen bonds are represented by green dashed lines. Hydrogen atoms are omitted for clarity.

With respect to the monoclinic structures at 100 and 170 K, it is well known that the unit cell is larger when the spin state of Fe^{II} centers changes from LS to HS with an approximately 3–4% increase in the cell volume from the primary cell in the LS state. In this context, it was found that the unit cell volume of **1-HT** in the high temperature HS phase increased by $\sim 74 \text{ \AA}^3$ (ca. 3%). This change in the **1-HT** unit cell volume is similar to those previously reported for Fe^{II} complexes bearing N₂O tridentate ligands, which exhibited complete SCO behavior.^{14, 20, 21}

According to previous studies,^{10, 11, 22, 23} a short intermolecular contact is known to correlate with the cooperative nature of SCO, whereas the weak interaction effects of the P4AE and π – π interactions are possibly responsible for the exceptionally high spin-transition temperatures and/or different hysteresis behaviors in the SCO complexes of [Fe^{II}(qsal-X)₂]. It was therefore considered that weak interaction effects, such as hydrogen bonding in the crystal structure, can be attributed to the N₂O Schiff base ligand present in these iron(II) SCO complexes. Moreover,

even if the octahedral coordination around the Fe^{II} atom in the [Fe^{II}(qsal-X)₂] molecule is distorted, the coordination environment must be anisotropic for SCO behavior to occur.

CONCLUSIONS

Iron(II) atom complexes consisting of N₂O Schiff base ligands have been found to exhibit various magnetic properties with spin crossover (SCO) behavior. In this work, the crystal packing of complexes **1-RT** and **1-HT** (prepared at room temperature and 323 K, respectively) containing carboxyl groups on their qsal-X ligands, (i.e., [Fe^{II}(qsal-COOH)₂]), were found to differ completely from those of previously reported [Fe^{II}(qsal-X)₂] complexes. In general, these groups are more likely to form hydrogen bonds than other X substituents, and so in the crystal packing of complex **1-HT**, hydrogen bonds between the salicylaldehyde moieties dominate the intermolecular interactions. In contrast, in the crystal packing of complex **1-RT**, hydrogen bonds between the hydrogen atoms of the hydroxyl group of the methanol solvent molecules and the oxygen atoms of the hydroxyl and carboxyl groups in salicylaldehyde dominate the intermolecular interactions. This can be understood by considering the dihedral angles of quinoline and the salicylaldehyde residues present in **1-HT** and **1-RT**, which are significantly distorted. Thus, intermolecular interactions occur through π - π interactions between the quinoline rings of the qsal-COOH ligands. For complex **1-HT**, these weak interaction effects produce the unique SCO behavior with a wide hysteresis >20 K. In contrast, complex **1-RT** does not exhibit SCO behavior, despite the possible presence of weak interactions between the [Fe^{II}(qsal-COOH)₂] molecules. These results therefore indicate that the key factors to achieving SCO behavior are the coordination environments of the Fe^{II} atoms resulting from different crystal packings and intermolecular interactions. In other words, the Fe^{II} atom is the inversion center of the [Fe^{II}(qsal-COOH)₂] molecule in **1-RT**, which is dependent on the crystallographic molecular

symmetry. Presumably, one of the reasons why **1-RT** does not show SCO behavior is that the distorted coordination environments around the Fe^{II} atoms are not anisotropic. In previous studies, [Fe^{II}(qsal-X)₂] complexes (X = Cl, Br, I, or COOH) were found to exhibit abrupt SCO properties at high temperatures, in contrast to their Fe^{III} analogs [Fe^{III}(qsal-X)₂](anion). In many cases, [Fe^{II}(qsal-X)₂] complexes exhibit various advantages as switchable materials, and so the precise design of their magnetic properties is of importance. In this context, we found that the inclusion of solvents in the crystal structure is necessary, as the solvent molecules can influence the interactions between the [Fe^{II}(qsal-X)₂] molecules. In the family of [Fe^{II}(qsal-X)₂] complexes, the presence of halogen substituents in the qsal-X moiety is effective in yielding SCO properties via π - π and P4AE (parallel fourfold aryl embrace) interactions. Our results therefore indicate that hydrogen bonding is also effective in producing SCO properties. Thus, Fe^{II} complexes consisting of Schiff bases containing N₂O donors have the potential to exhibit a variety of magnetic properties owing to differences in the formed 3D networks. In conclusion, for the design of a potential SCO material, the fundamental requirement necessary to achieve an abrupt SCO in Fe-qsal complexes is a combination of weak interaction effects, such as π - π , P4AE, and hydrogen bonding interactions. Furthermore, the SCO properties can be produced by designing the coordination environment around the Fe^{II} atoms to be both distorted and anisotropic. In the future, we will conduct to clarify the correlation between SCO behavior and weak interaction in structure by solvent exchange for the family of [Fe^{II}(qsal-X)₂] complexes.

ASSOCIATED CONTENT

Supporting Information: Supporting Information is available free of charge at

<https://pubs.acs.org/doi/10.1021/acs.cgd.xxxxxx>. Crystallographic information and figures (PDF).

Accession Codes: CCDC 2024556, 2073267, 2073268, and 2073269 contain the supplementary crystallographic data for this study. These data can be obtained free of charge via www.ccdc.cam.ac.uk/data_request/cif, or by emailing data_request@ccdc.cam.ac.uk, or by contacting The Cambridge Crystallographic Data Centre, 12 Union Road, Cambridge CB2 1EZ, UK; fax: +44 1223 336033.

AUTHOR INFORMATION

Corresponding Author

Kunihisa Sugimoto—Diffraction & Scattering Division, Japan Synchrotron Radiation Research Institute (JASRI), 1-1-1 Kouto, Sayo-cho, Sayo-gun, Hyogo 679-5198 Japan; Institute for Integrated Cell-Material Sciences (iCeMS), Institute for Advanced Study, Kyoto University, Yoshida-Honmachi, Sakyo-ku, Kyoto 606-8501 Japan

e-mail: ksugimoto@spring8.or.jp, sugimoto.kunihisa.4s@kyoyo-u.ac.jp

Authors

Takashi Okubo, Department of Chemistry, Faculty of Science and Engineering, Kindai University, Higashi-Osaka, Osaka 577-8502, Japan

Maekawa Masahiko, Department of Chemistry, Faculty of Science and Engineering, Kindai University, Higashi-Osaka, Osaka 577-8502, Japan

Takayoshi Kuroda-Sowa, Department of Chemistry, Faculty of Science and Engineering, Kindai University, Higashi-Osaka, Osaka 577-8502, Japan

Author Contributions

The manuscript was written through contributions of all authors. All authors have given approval to the final version of the manuscript.

Funding Sources

This work was supported by a JSPS KAKENHI grant (No. 16H06514 (Coordination Asymmetry)).

ACKNOWLEDGMENT

Synchrotron radiation X-ray diffraction measurements were carried out at the SPring-8 facility in Japan (Proposal Nos. 2017B1254, 2018A1426, 2018B1409, 2018B1412, and 2018B1818). We thank Ms. Kana Kimura and Mr. Atsushi Hinano for their help with the experiments.

ABBREVIATIONS

SCO, spin crossover; HS, high spin; LS, low spin; qsal, *N*-(8'-quinolyl)-2-hydroxy-1-salicylaldimine; P4AE, parallel four-fold aryl embrace interactions.

REFERENCES

1. Abu-Dief, A. M.; Mohamed, I. M. A. A Review on Versatile Applications of Transition Metal Complexes Incorporating Schiff Bases. *Beni Suef Univ. J. Basic Appl. Sci.* **2015**, *4* (2), 119–133.

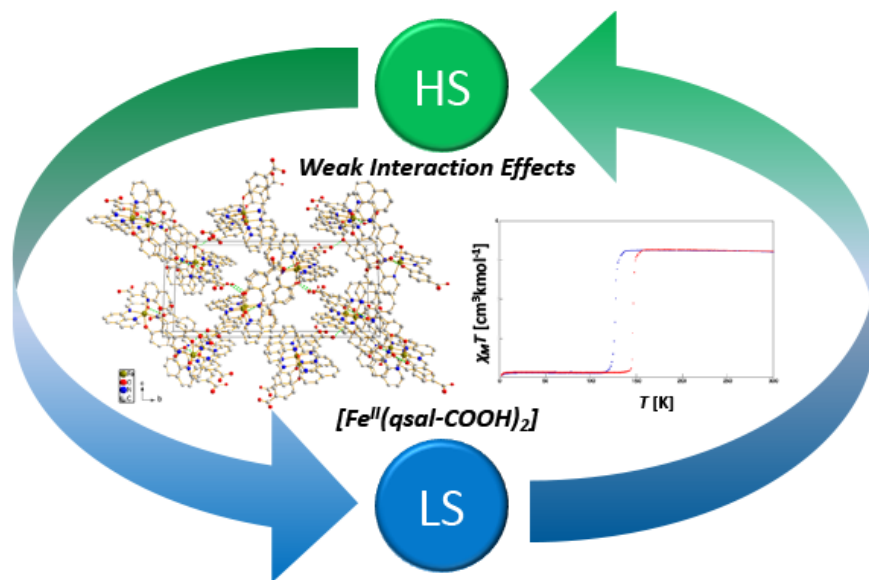
2. Gütlich, P.; Jung, J.; Goodwin, H. A. Spin Transitions in Iron(II) Complexes. In, Coronado, E., Delhaès, P., Gatteschi, D., Miller, J. S., Eds. *Molecular Magnetism: from Molecular Assemblies to the Devices*; Springer Netherlands: Dordrecht, 1996, pp 327–378.
3. Gütlich, P. Spin Crossover in Iron(II)-Complexes. *Metal Complexes*; Springer, 1981; pp 83–195.
4. Goodwin, H. A. Spin Transitions in Six-Coordinate Iron(II) Complexes. *Coord. Chem. Rev.* **1976**, *18* (3), 293–325.
5. Michalowicz, A.; Moscovici, J.; Ducourant, B.; Cracco, D.; Kahn, O. EXAFS and X-Ray Powder Diffraction Studies of the Spin Transition Molecular Materials [Fe(Htrz)₂(trz)](BF₄) and [Fe(Htrz)₃](BF₄)·2H₂O (Htrz = 1,2,4-4H-triazole; trz = 1,2,4-triazolato). *Chem. Mater.* **1995**, *7* (10), 1833–1842.
6. Haasnoot, J. G.; Groeneveld, W. L. Complexes of 1,2,4-Triazoles, VII [1] Preparation and Vibrational Spectra of 4,4'-Bi-1,2,4-Triazole and Some of Its Complexes with Transition Metal (II) *Thiocyanates*. *Z. Naturforsch.* **1979**, 1500–1506; Vol. 34b.
7. Psomas, G.; Bréfuel, N.; Dahan, F.; Tuchagues, J. P. An Unprecedented Trinuclear Structure Involving Two High-Spin and One Spin-Crossover Iron(II) Centers. *Inorg. Chem.* **2004**, *43* (15), 4590–4594.
8. Zhong, Z. J.; Tao, J.-Q.; Yu, Z.; Dun, C.-Y.; Liu, Y.-J.; You, X.-Z. A Stacking Spin-Crossover Iron(II) Compound with a Large Hysteresis. *J. Chem. Soc. Dalton Trans.* **1998**, (3), 327–328.
9. Gallois, B.; Real, J. A.; Hauw, C.; Zarembowitch, J. Structural Changes Associated with the Spin Transition in bis(Isothiocyanato)Bis(1,10-Phenanthroline)Iron: a Single-Crystal X-Ray Investigation. *Inorg. Chem.* **1990**, *29* (6), 1152–1158.

10. Phonsri, W.; Macedo, D. S.; Vignesh, K. R.; Rajaraman, G.; Davies, C. G.; Jameson, G. N. L.; Moubaraki, B.; Ward, J. S.; Kruger, P. E.; Chastanet, G.; Murray, K. S. Halogen Substitution Effects on N₂O Schiff Base Ligands in Unprecedented Abrupt Fe^{II} Spin Crossover Complexes. *Chemistry* **2017**, *23* (29), 7052–7065.
11. Phonsri, W.; Davies, C. G.; Jameson, G. N. L.; Moubaraki, B.; Ward, J. S.; Kruger, P. E.; Chastanet, G.; Murray, K. S. Symmetry Breaking Above Room Temperature in an Fe(ii) Spin Crossover Complex with an N₄O₂ Donor Set. *Chem. Commun. (Camb)* **2017**, *53* (8), 1374–1377.
12. Kuroda-Sowa, T.; Isobe, R.; Yamao, N.; Fukumasu, T.; Okubo, T.; Maekawa, M. Variety of Spin Transition Temperatures of Iron(II) Spin Crossover Complexes with Halogen Substituted Schiff-Base Ligands, Hqsal X (X = F, Cl, Br, and I). *Polyhedron* **2017**, *136*, 74–78.
13. Kuroda-Sowa, T.; Kimura, K.; Kawasaki, J.; Okubo, T.; Maekawa, M. Effects of Weak Interactions on Spin Crossover Properties of Iron(II) Complexes with Extended π -Conjugated Schiff-Base Ligands. *Polyhedron* **2011**, *30* (18), 3189–3192.
14. Kuroda-Sowa, T.; Yu, Z.; Senzaki, Y.; Sugimoto, K.; Maekawa, M.; Munakata, M.; Hayami, S.; Maeda, Y. Abrupt Spin Transitions and LIESST Effects Observed in FeII Spin-Crossover Complexes with Extended π -Conjugated Schiff-Base Ligands Having N₄O₂ Donor Sets. *Chem. Lett.* **2008**, *37* (12), 1216–1217.
15. Sheldrick, G. M.; SHELXT. *Acta Crystallogr. A Found. Adv.* **2015**, *71* (1), 3–8.
16. Sheldrick, G. M. Crystal Structure Refinement with SHELXL. *Acta Crystallogr. C Struct. Chem.* **2015**, *71* (1), 3–8.
17. Dolomanov, O. V.; Bourhis, L. J.; Gildea, R. J.; Howard, J. A. K.; Puschmann, H. OLEX2: a Complete Structure Solution, Refinement and Analysis Program. *J. Appl. Crystallogr.* **2009**, *42* (2), 339–341.

18. Hübschle, C. B.; Sheldrick, G. M.; Dittrich, B. ShelXle: a Qt Graphical User Interface for SHELXL. *J. Appl. Crystallogr.* **2011**, *44* (6), 1281–1284.
19. Zhang, L.; Xu, G.-C.; Wang, Z.-M.; Gao, S. Two Mononuclear Iron(II) Spin-Crossover Complexes with a N₄O₂ Coordination Sphere. *Eur. J. Inorg. Chem.* **2013**, *2013* (5–6), 1043–1048.
20. Hill, S.; Datta, S.; Liu, J.; Inglis, R.; Milios, C. J.; Feng, P. L.; Henderson, J. J.; del Barco, E.; Brechin, E. K.; Hendrickson, D. N. Magnetic Quantum Tunneling: Insights from Simple Molecule-Based Magnets. *Dalton Trans.* **2010**, *39* (20), 4693–4707.
21. Pfaffeneder, T. M.; Thallmair, S.; Bauer, W.; Weber, B. Complete and Incomplete Spin Transitions in 1D Chain Iron(II) Compounds. *New J. Chem.* **2011**, *35* (3), 691–700.
22. Weber, B. Spin Crossover Complexes with N₄O₂ Coordination Sphere—the Influence of Covalent Linkers on Cooperative Interactions. *Coord. Chem. Rev.* **2009**, *253* (19–20), 2432–2449.

Table of Contents Entry for Visualization of Weak Interaction Effects on N₂O Schiff Base Ligands in Iron(II) Spin Crossover Complexes

Kunihisa Sugimoto^{†, ‡*}, Takashi Okubo[§], Masahiko Maekawa[§], Takayoshi Kuroda-Sowa[§]



SYNOPSIS

A single crystal of an iron(II) spin crossover (SCO) complex containing an N₂O Schiff base ligand (i.e., [Fe^{II}(qsal-COOH)₂]) were successfully visualized by structural analyses. The fundamental requirements for an abrupt SCO, particularly in Fe-qsal complexes, are not only a combination of weak interaction effects, but also the presence of solvents in the crystal structure, as solvent molecules can influence the interactions between the [Fe^{II}(qsal-X)₂] molecules.